Ninth Canadian Conference on
Earthquake Engineering
Ottawa, Ontario, Canada
26-29 June 2007

DUCTILITY AND STRENGTH ASSOCIATED WITH CONFINEMNT IN CONCRETE-FILLED FRP TUBES

A. Z. Fam[1]

ABSTRACT

This paper discusses ductility and strength aspects of concrete-filled fibre-reinforced polymer (FRP) circular tubes (CFFTs) under axial loads and in flexure. The effects of tube thickness, concrete strength and size of a central hole that may be used to reduce self weight are examined for axial members. For flexural members, the contributions of FRP tube and steel reinforcement are assessed by comparing a steel-reinforced CFFT to a regular unreinforced CFFT and a reinforced specimen without a tube. The effects of tube laminate structure, concrete strength, and steel reinforcement ratio are examined. It is shown that FRP tubes provide substantial enhancement to strength and ductility under axial loads due to confinement, however, to avoid strain softening and maintain at least a plastic behavior, there is a minimum tube thickness that should be used and a maximum diameter for the central hole. It is recommended to fill the tubes with low strength concrete as it leads to higher confinement effectiveness and ductility, than high strength concrete. In flexure, steel-reinforced CFFTs showed superior performance to both unreinforced CFFTs and reinforced members without a tube. The tube prevents concrete cover spalling and buckling of rebar, leading to developing rebar plastic capacity, and thereby gaining large ductility. The tube fails progressively, accompanied by several load drops, providing several warning signs.

Introduction

Concrete-filled FRP tubes (CFFTs) offer numerous advantages from simplicity of construction and durability points of view. The non-permeable and non-corrosive tube protects the concrete core from the damaging effect of freeze-thaw cycles (Kong 2005), and the internal rebar, if used, from corrosion. The tube is essentially a structural form for casting the concrete core (Seible 1996). It usually has several layers of fibers oriented at various angles to provide strength and stiffness in the longitudinal and circumferential directions. A major advantage of the tube is concrete confinement, where the tube controls the transverse dilation and expansion of the concrete core under axial compression, which increases the concrete strength and ductility substantially. Unlike steel tubes or spirals, which exhibit a constant confining pressure once the steel yields, the confinement pressure of the FRP tube continuously increases as the FRP material is linear elastic till failure (Mirmiran et al 1997). The tube is also more effective than conventional steel spirals as the tube confines the entire section, whereas the spiral confines the inner core of the section only and the concrete cover is usually susceptible to cracking and

[1]Associate Professor and Canada Research Chair in Innovative and Retrofitted Structures, Dept. of Civil Engineering, Queen's University, Kingston, ON, K7L 3N6

spalling (Cole and Fam 2006).

CFFTs are quite effective in a number of applications, including bridge piers, piles, and mono poles and have already been employed in some of these applications (Fam et al 2003a) and (Fam et al 2003b). Due to the superior confinement effectiveness of the tubes, CFFTs have excellent ductility and large deformation capacity before failure, and as such, they could be quite effective in applications in seismic regions, particularly for bridge piers.

This paper summarizes various aspects of the CFFT system related to strength and ductility under axial loads and in flexure, selected from several studies conducted by the author over the past ten years.

Experimental Program

The experimental study included testing of CFFT members under axial compression as short columns and in bending as simply supported beams. A summary of the experimental work is provided next.

FRP Tubes

Several glass-fibre reinforced polymer (GFRP) tubes were used in the fabrication of test specimens. The tubes were fabricated using the filament-winding technique and had about 51percent fibre volume fraction. The filament-winding process employed standard E-glass roving wound around a cylindrical mandrel. To facilitate removal of the tubes from the mandrel, a thin liner was provided at the inner surface of the tubes, which is not considered part of the structural wall thickness. The tubes included layers of fibres oriented in both the longitudinal and circumferential directions at small angles. Table 1 shows a summary of the various properties of the tubes, including outer diameter, structural wall thickness, tensile strengths in the hoop and longitudinal direction (calculated based on classical lamination theory) and the laminate structure, including fiber orientations of different layers with respect to the longitudinal direction.

Table 1. General description of the GFRP tubes.

Tube ID	O.D. (mm)	Thickness (mm)	f_u (Ten.) Hoop (MPa)	f_u (Ten.) Long. (MPa)	Laminate structure
T1	100	3.08	398	480	[-88/+3/-88/+3/-88/+3/-88/+3/-88]
T2	168	2.56	547	348	[+8/-86/-86/+8/-86/+8/-86/+8/-86]
T3	219	2.21	536	318	[+15/-82/-82/+15/-82/+15/-82/+15/-82]
T4	326	6.4	401	N/A	[-88/+3/-88/-88/+3/-88/+3/-88/+3/-88]
T5	219	3.2	N/A	160	[-88/+5/-88/-88/+5/-88/+5/-88]

Axial CFFT Members

Eight concrete-filled GFRP tubes (CFFTs) C1 to C8, of various sizes, tubes, concrete strengths and cross-sectional configurations, were tested under axial compression as short columns. Table 2 provides a summary of the test specimens, including the tube type, which is given in Table 1, outer diameter, inner diameter for specimens with a central hole, the unconfined compressive strength of the concrete fill, and test results in terms of confinement ratio and ductility, which will be discussed later. The central holes were maintained during casting using cardboard tubes. Specimen C1 is intended to establish the general shape of axial load-strain curve of the CFFT system in compression and examine the effect of GFRP tube on the ductility. Specimens C2 to C6 are used to examine the effect of the size of the central hole on the strength and ductility of the CFFT system. Specimens C7 and C8 are used to examine the effect of the strength of the concrete fill on the overall strength and ductility of the CFFT system.

Flexural CFFT Members

Three beam specimens B1 to B3 were tested in flexure, using four-point bending configuration. Specimen B1 was a control specimen without GFRP tube but was reinforced by 6-15M longitudinal steel rebar. Specimen B2 was a CFFT fabricated using GFRP tube T3 but without any steel reinforcement. Specimen B3 was also a CFFT specimen fabricated using tube T5 but included 6-15M longitudinal steel rebar. The steel reinforcement was placed in an axi-symmetric pattern within the cross-section. The yield and ultimate strengths of the steel rebar were 425 and 680 MPa, respectively. Table 3 provides a summary of test specimens, including the tube used (from Table 1), diameter, span, steel reinforcement, concrete strength and the measured moment capacity.

Table 2. Summary of the axial CFFT members' properties.

Specimen ID	Tube ID	O.D. (mm)	I.D. (mm)	Height (mm)	f_c' (MPa)	f_{cc}' (MPa)	f_{cc}' / f_c'	Ductility ($\varepsilon_u / 0.003$)
C1	T1	100	-	200	37	81	2.19	3.67
C2	T2	168	-	336	58	97	1.67	4.43
C3	T2	168	95	336	58	78	1.34	4.17
C4	T3	219	-	438	58	70	1.21	3.37
C5	T3	219	95	438	58	61	1.05	2.90
C6	T3	219	133	438	58	56	0.97	2.40
C7	T4	326	-	652	26	58	2.22	2.13
C8	T4	326	-	980	60	67	1.12	1.60

Table 3. Summary of the CFFT and control beam properties.

Specimen ID	Tube ID	O.D. (mm)	Span (m)	Steel rebar	f_c' (MPa)	M_u (kN.m)
B1	T3	219	2.9	-	58	18
B2	-	203	2.2	6-15M	39	37
B3	T5	219	2.2	6-15M	39	60

Experimental Results

Axial CFFT Members

Figure 1 shows the load-axial strain behavior of specimen C1. Also shown in the same figure are the load-axial strain responses of the plain concrete core, tested using a standard 150x300 mm cylinder, and the hollow FRP tube T1 tested in compression. The figure clearly shows that the plain concrete reaches a peak strength and then the curve descends rapidly at a rate depending on the rate of loading and concrete strength until concrete crushes, as shown in Fig. 4(a). For the FRP tube, the behavior is linear elastic till failure, which occurred prematurely at the end of the tube, as a result of the brooming effect shown in Fig. 4(b). The behavior of CFFT C1, however, reflects a substantial increase in the total strength and ductility as reflected by the large strain at failure and the strain hardening response. The capacity of the hybrid system is substantially larger than the sum of capacities of the individual components due to the confinement mechanism, and the behavior is very ductile, despite the fact that the individual components are brittle. A ductility definition is introduced, as the ratio of axial strain at failure to the typical strain of plain concrete at failure, taken as 0.003. As such, the ductility of specimen C1 is 3.67 and the confinement ratio, defined as the ratio of confined concrete strength f_{cc}' to the unconfined concrete strength f_c', is 2.19, as shown in Table 2. Failure of C1 occurred by fracture of the tube in the hoop direction, as shown in Fig. 4(c), under hoop tensile stresses resulting from the confinement effect,

combined with axial compressive stresses in the tube. More details on this behavior can be found in Fam and Rizkalla (2001a).

Figure 2 shows the axial load-strain behavior of the specimens C2 to C6 with different central holes sizes. Table 2 also shows the confined concrete strength, confinement ratio and ductility ratio of the specimens. It is quite clear that the presence of a central hole reduces the confinement ratio relative to a totally-filled tube. It also reduces the ductility ratio slightly. Failure occurred for all the specimens in a similar manner to C1, as shown in Fig. 4(d) for C2. Further details on the effect of the central hole can be found in Fam and Rizkalla (2001).

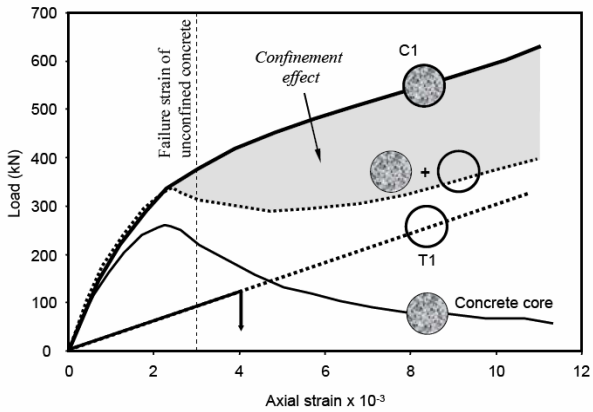

Figure 1. Load-strain behavior of specimen C1 as compared to individual components.

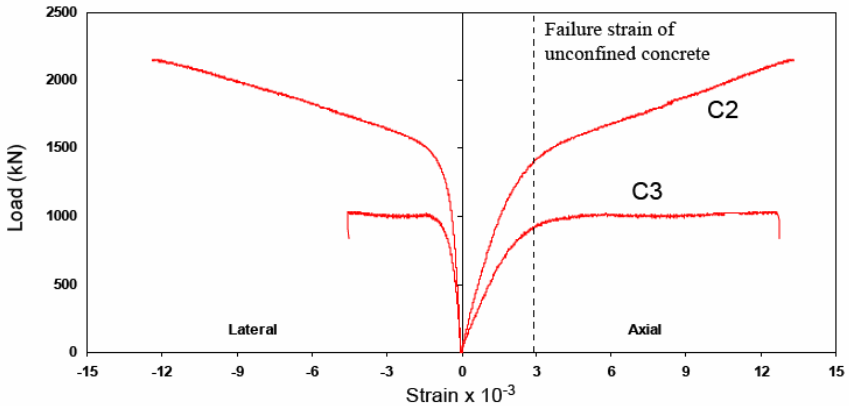

(a) Specimens C2 and C3

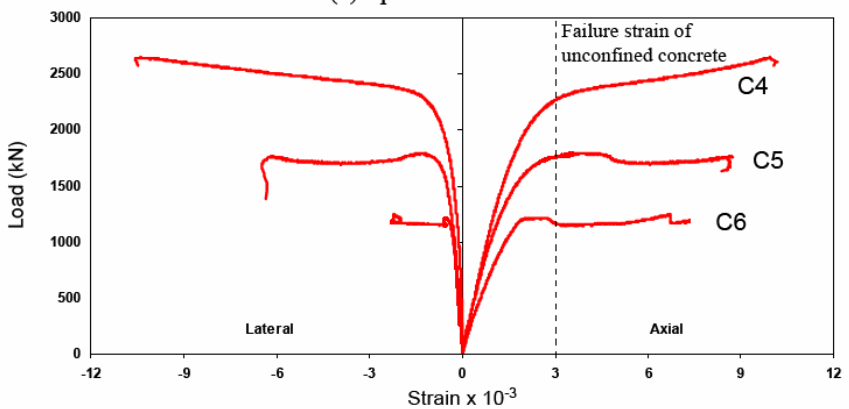

(b) Specimens C4, C5 and C6

Figure 2. Stress-strain behavior of specimens of different tubes and central hole sizes.

The effect of the strength of the concrete core is shown in Fig. 3. Both specimens C7 and C8 have the same FRP tube but different values of the unconfined concrete strength of the core. It is clear that as the concrete strength increased from 26 MPa to 60 MPa, the confinement effectiveness reduced from 2.12 to 1.12 and the ductility reduced from 2.13 to 1.6. This is a result of the lower dilation capacity of high strength concrete relative to low strength concrete. As a result, the confinement effectiveness of low strength concrete is higher than that for high strength concrete. Additional details on this behavior can be found in Mandal et al (2003).

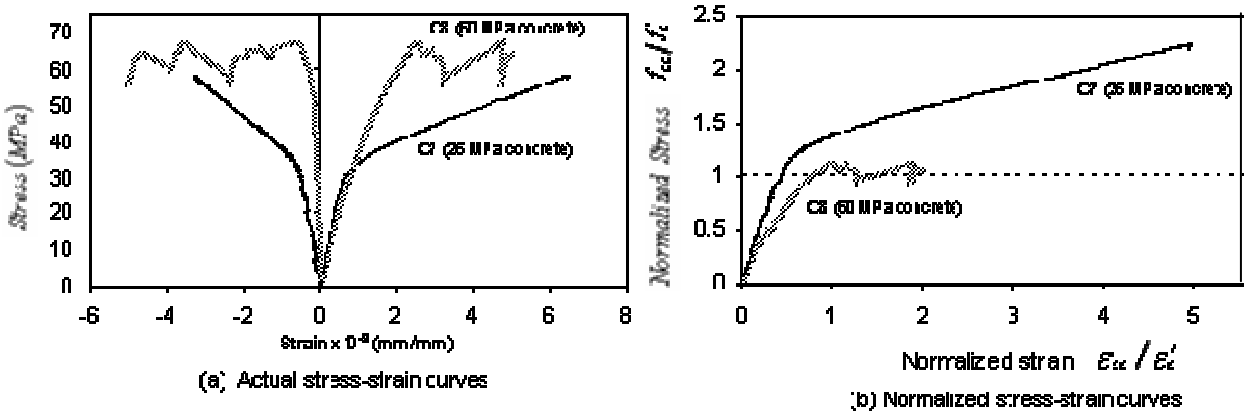

Figure 3. Effect of unconfined concrete strength on strength and ductility of CFFTs.

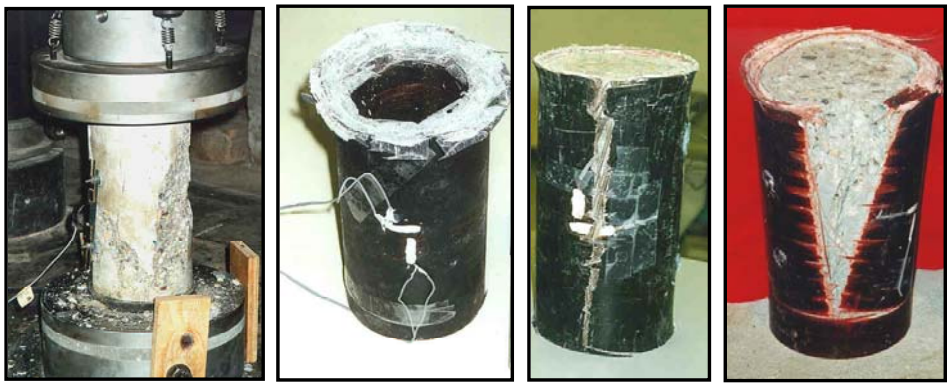

(a) Plain concrete (b) Hollow GFRP Tube 1 (c) CFFT C1 (d) CFFT C2

Figure 4. Failure modes of plain concrete, hollow GFRP tube, and CFFTS under axial loads.

Flexural CFFT Members

Figure 5(a) shows the typical load-deflection response of CFFT members based on specimen B1. The behavior is bi-linear with a stiffness reduction after first cracking. Failure occurred by fracture of the GFRP tube at the tension side as shown in Fig. 6(a). Once the tube failed, the beam completely collapsed. As such, the behavior is non-ductile and is essentially linear elastic. Unlike axial CFFT members, there is little confinement effect in CFFT flexural members failing in tension (Fam and Rizkalla 2003).

Figure 5(b) shows the load-deflection behavior of specimens B2 and B3, both with the same longitudinal steel reinforcement but B3 has an FRP tube, whereas B2 doesn't. The behavior of B2 shows very limited ductility and strength relative to B3. Once the concrete cover crushes and spalls in compression, the load

drops gradually until the steel rebar buckles in compression, as shown in Fig. 6(b). Before concrete crushing and spalling, the behavior doesn't reflect any ductility since the steel reinforcement is placed in an axi-symmetric pattern, and as such, not all layers of rebar yields simultaneously. On the other hand, beam B3 demonstrated a substantially higher strength and ductility, as a result of the FRP tube. In this case the tube contributes as a longitudinal and transverse reinforcement and confines the concrete cover, preventing spalling. The tube failed first in longitudinal tension as shown in Fig. 6(a) and the load drops slightly but then rises again as a result of the internal reinforcement and the intact part of the tube in compression. Then, the tube crushed gradually in compression, as shown in Fig. 6(c), where the load also drops gradually to a load level higher than that of control specimen B2. The beam continues to deflect at that sustained high load, until eventually the tube fractures under hoop tensile stresses, as shown in Fig. 6(d), due to the confinement pressure. The load then drops to a load level similar to that of B2. It is clear that the FRP tube results in a progressive sequential failure with several warning signs. It also prevents concrete cover crushing and spalling and prevents rebar buckling in compression. This allows the steel reinforcement to develop its plastic capacity, which enhances ductility substantially. By comparing the behavior of B1, B2 and B3, it is clear that adding some steel reinforcement to the CFFT system in flexure provides substantial improvements in behavior, particularly with regard to ductility. This behavior is superior to that of normal CFFTs or reinforced concrete beam without a GFRP tube. Further details on this behavior can be found in Cole and Fam (2006).

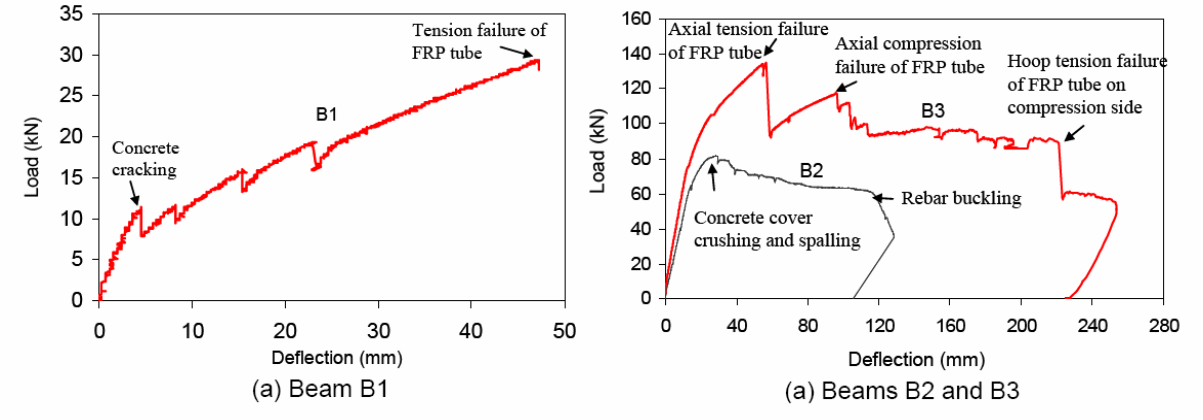

(a) Beam B1 (a) Beams B2 and B3

Figure 5. Load-deflection behavior of CFFT test beams.

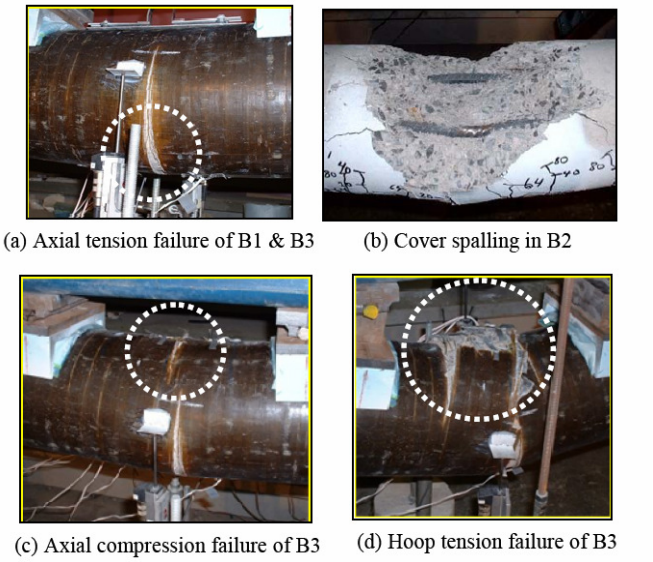

(a) Axial tension failure of B1 & B3 (b) Cover spalling in B2

(c) Axial compression failure of B3 (d) Hoop tension failure of B3

Figure 6. Failure modes of control and CFFT test beams.

Analytical Modeling and Parametric Studies

Axial Members

A confinement model has been developed using the concepts of equilibrium and radial displacement compatibility at the interface between the concrete core and the FRP tube. The model accounts for the effect of axial load applied to the concrete core only or to the concrete and FRP tube. The model also accounts for FRP tubes of different laminate structures and the central hole size. Details of the model can be found elsewhere (Fam and Rizkalla 2001(b)). The model was verified using test results and showed good agreement, as shown in Fig. 7(a).

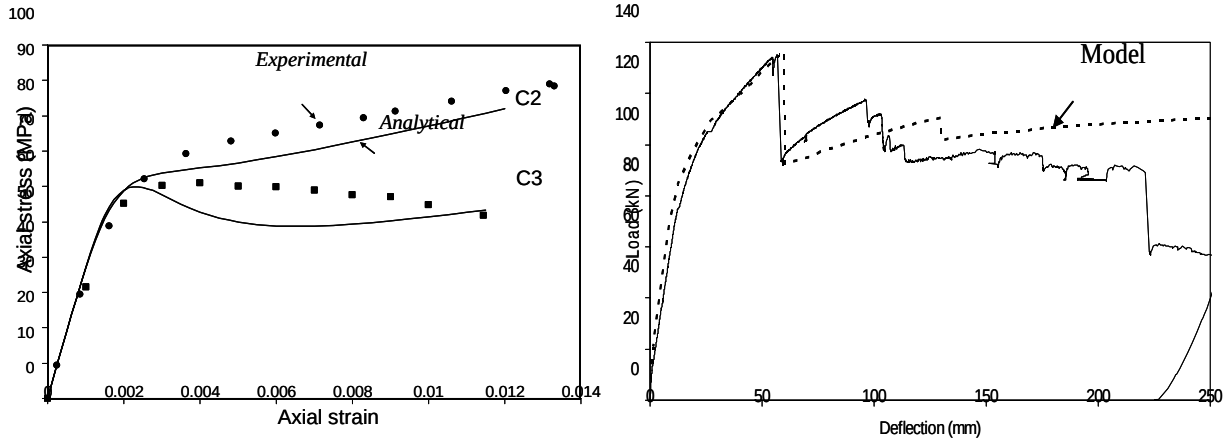

(a) Axial CFFT members (b) Flexural CFFT members

Figure 7. Verification of analytical models using test results.

The model was then used in a parametric study to examine the effects of various parameters on the stress-strain curve of a 150 mm diameter CFFT with a GFRP tube of fibres oriented in the hoop direction and filled with 40 MPa concrete. Figure 8(a) shows that increasing the tube thickness from 0.5 to 8 mm has increased the strength from 40 to 97 MPa, however, the strain at failure did not change much and the ductility in general was about 4.7. It is noted, however, that the descending part of the concrete curve rises gradually as the tube thickness increases, such that the ultimate strength at failure increases from a value lower than f_c' up to a value f_{cc}' higher than f_c'. In this case, it is clear that at least a 0.5 mm thick tube is needed to achieve a plastic behavior and avoid strain softening.

Figure 8(b) shows that as the central hole size increases from 25 to 125 mm, the ultimate strength reduces from 61 to 14 MPa, which is lower than the f_c' value of 40 MPa. However, the strain at failure, and hence ductility, remain unchanged. It is also noted that to achieve a plastic behavior and avoid strain softening, the hole size should not exceed 100 mm in this case (i.e. inner-to-outer diameter ratio of 0.6).

Figure 8(c) shows the effect of applying the load over the concrete core and the tube. It results in reducing the confinement ratio from 3.1 to 1.65. The ultimate strain is also reduced substantially, and hence the ductility is reduced from 12.5 to 4.6. This is a result of the tube being subjected to axial compressive stresses in addition to the hoop tensile stresses, which weakens the tube in the hoop direction substantially.

Flexural Members

A 'cracked section analysis' model was developed using the concepts of equilibrium and strain compatibility to establish the load-deflection responses of steel-reinforced CFFTs. The model is capable of predicting the post-failure response and capturing the progressive failure. Details of the model can be

found elsewhere (Cole and Fam 2006). The model was verified as shown in Fig. 7(b) and showed good agreement. It was then used in a parametric study to examine the effects of tube laminate structure, concrete strength and steel reinforcement ratio, as shown in Fig. 8(d, e and f). Figure 8(d) shows that increasing the proportion of fibers in the longitudinal direction of the tube (for the same thickness) results in increasing the flexural capacity but has no effect on the post-failure residual strength or ductility. Figure 8(e) shows that increasing the concrete strength results in some increase in the flexural capacity but larger increase in the post-failure residual strength. It, however, reduces ductility slightly. Figure 8(f) shows that increasing the steel reinforcement ratio substantially increases the flexural strength, residual capacity and ductility. It is also noted that the residual strength level approaches that of the peak strength as the steel ratio increases. For the case of zero steel ratio, the behavior is quite brittle and the load drops completely upon tension failure of the tube, which is quite similar to the behavior of beam B1 in Fig. 5(a).

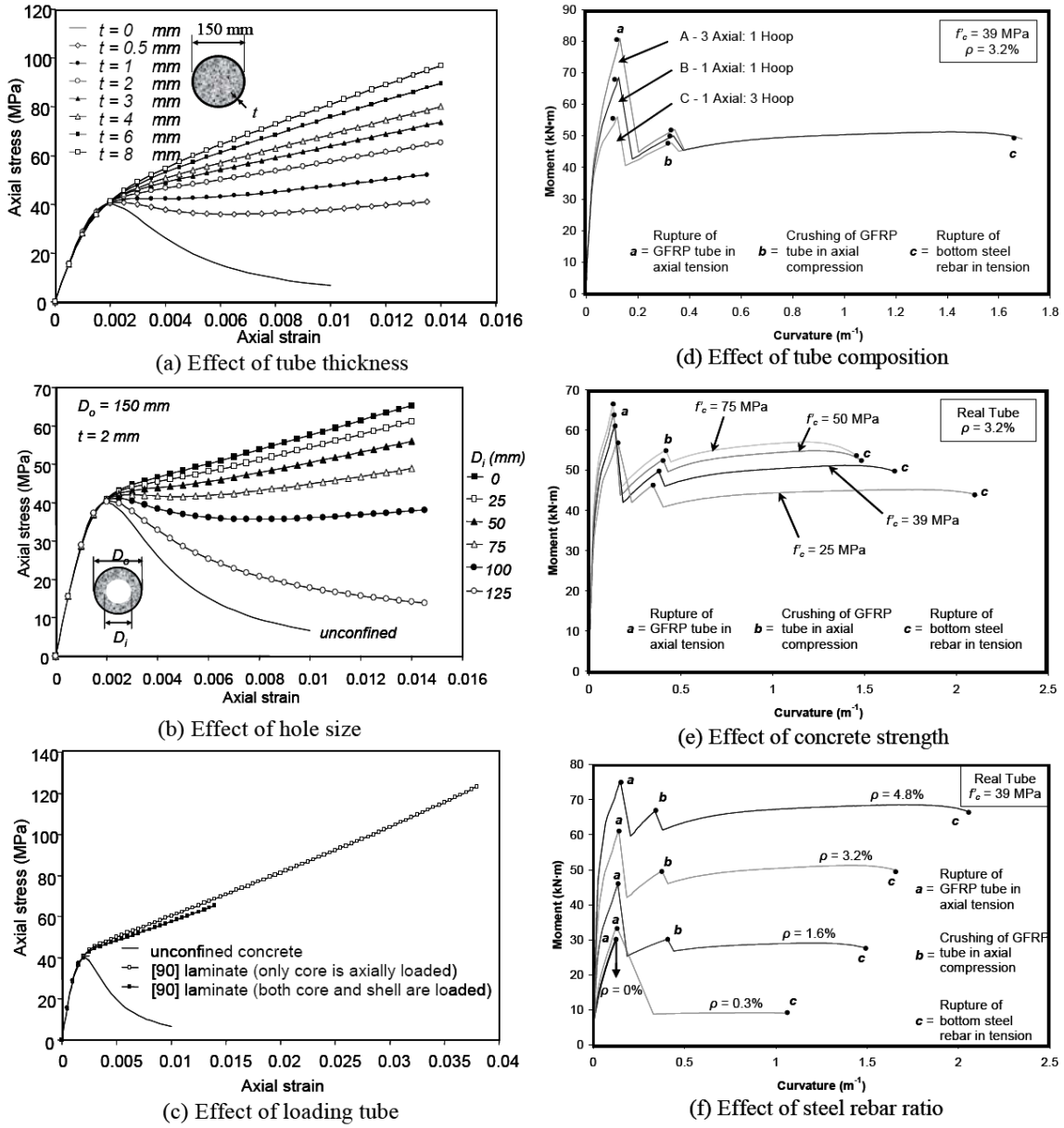

Figure 8. Summary of results of the parametric studies for axial and flexural CFFT members.

Conclusions

The following conclusions are drawn from the experimental and parametric studies:

1. FRP tubes increase the strength and ductility of axial CFFT members due to confinement. CFFT flexural members on the other hand are quite brittle
2. There is a minimum tube thickness necessary to avoid strain softening by maintaining a plastic behavior in axial CFFT members. Thicker tubes will lead to a strain hardening behavior.
3. There is a maximum hole size that should not be exceeded in the concrete core, otherwise strain softening may occur in axial CFFT members.
4. Applying axial load on the tube reduces strength and ductility of CFFT members.
5. Filling FRP tubes with low strength concrete results in substantially better ductility and ultimate axial strength, than using high strength concrete fill.
6. Adding a moderate steel reinforcement ratio to CFFT flexural members increases their ductility substantially. They fail progressively with several warning signs.
7. Increasing the percentage of fibers in the longitudinal direction of the tube results in increasing the flexural capacity but has no effect on the post-failure residual strength or ductility.

Acknowledgement

The author wishes to acknowledge the financial support provided by the ISIS Canada research network

References

Cole, B. and Fam, A., 2006. Flexural Load Testing of Concrete-Filled FRP Tubes with Longitudinal Steel and FRP Rebar, *Journal of Composites for Construction*, 10(2):161-171.

Fam, A. Z. and Rizkalla, S. H., 2001a. Behavior of Axially Loaded Concrete-Filled Circular Fiber Reinforced Polymer Tubes, *ACI Structural Journal*, 98(3):280-289.

Fam, A. Z. and Rizkalla, S. H., 2001b. Confinement Model for Axially Loaded Concrete Confined by FRP Tubes, *ACI Structural Journal*, 98(4):251-461.

Fam, A. Z. and Rizkalla, S. H., 2002. Flexural Behaviour of Concrete-Filled Fiber-Reinforced Polymer Circular Tubes, *Journal of Composites for Construction*, 6(2):123-132.

Fam, A., Pando, M., Filz, G. and Rizkalla, S., 2003a. Precast Composite Piles for the Route 40 Bridge in Virginia Using Concrete-Filled FRP Tubes, *PCI Journal*, 48(3):32-45.

Fam, A., Greene, R. and Rizkalla, S., 2003b. Field Applications of Concrete-Filled FRP Tubes for Marine Piles, Field Application of FRP Reinforcement: Case Studies, ACI Special Publication, SP-215-9:161-180.

Kong, A., 2005. Freeze-Thaw Behavior of Concrete Confined by FRP when Simultaneously Subjected to Sustained Axial Loads. M.Sc. Thesis, Department of Civil Engineering, Queen's University, pp.210.

Seible, F., 1996. Advanced Composite Materials for Bridges in the 21st Century. Proc., of the Advanced Composite Materials in Bridges and Structures, M. El-Badry, editor, published by CSCE, Montreal, pp.17-30.

Mandal, S., Hoskin, A. and Fam, A., 2005. Influence of Concrete Strength on Confinement Effectiveness of Fiber-Reinforced Polymer Circular Jackets, *ACI Structural Journal*, 102(3):383-392.

Mirmiran, A., and Shahawy, M., 1997. Behavior of Concrete Columns Confined by Fiber Composites, *Journal of Structural Engineering*, May, pp. 583-590.